

1 *Review*

2 **Advances in non-destructive early assessment of fruit** 3 **ripeness towards defining optimal time of harvest** 4 **and yield prediction – a review**

5 **Bo Li¹, Julien Lecourt¹, Gerard Bishop^{1*}**

6 ¹ NIAB EMR, East malling, Kent, ME19 6BJ, UK

7 * Correspondence: Gerard.bishop@emr.ac.uk

8 **Abstract:** Global food security for the increasing world population not only requires increased
9 sustainable production of food but a significant reduction in pre- and post-harvest waste. The
10 timing of when a fruit is harvested is critical for reducing waste along the supply chain and
11 increasing fruit quality for consumers. The early in field assessment of fruit ripeness and
12 prediction of the harvest date and yield by non-destructive technologies have the potential to
13 revolutionize farming practices and enable the consumer to eat the tastiest and freshest fruit
14 possible. A variety of non-destructive techniques have been applied to estimate the ripeness or
15 maturity but not all of them are applicable for in situ (field or glasshouse) assessment. This review
16 focuses on the non-destructive methods which are promising, or have already been, applied to the
17 pre-harvest in field measurement including colorimetry, visible imaging, spectroscopy and
18 spectroscopic imaging. Machine learning and regression models used in assessing ripeness are
19 also discussed.

20 **Keywords:** Pre-harvest; ripeness; image analysis; machine learning; fruit phenotyping,
21

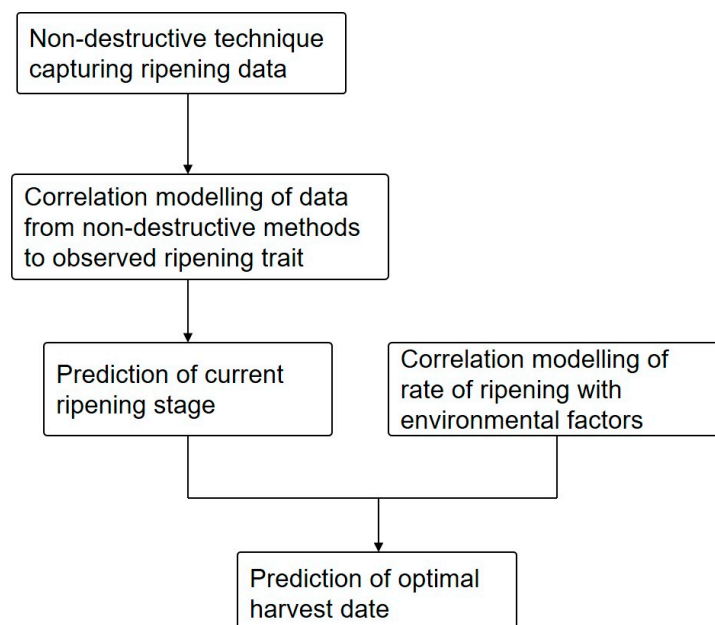
22 **1. Introduction**

23 There are many ways in which the status of global food security can be improved for the
24 world's increasing population. Increased fruit production through adding to the area cropped is not
25 sustainable and thus productivity per unit land area must be increased. Simultaneously there is a
26 need to prevent waste and for fruit production the timing of harvest is crucial to ensure production
27 meets the commercial ripeness specifications. Over- or under-ripe fruits have a lower or even no
28 retail value and represent a significant income loss and a waste of resources. For the consumer too
29 early harvest reduces the taste and quality of fruits whilst a late harvest can lead to reduced shelf
30 life, poor appearance, and "off" flavours and odours. The early in-field assessment of fruit ripeness
31 and the prediction of both harvest date and yield will therefore greatly reduce the waste in the
32 supply chain and thus help towards improving food security.

33 The non-destructive on-plant assessment of fruit ripeness has received increasing interest as it
34 provides several advantages compared with traditional destructive methods, such as high-
35 throughput assessment, simultaneous multiple measurements and real time decision making. The
36 phenotypic changes during fruit ripening are complex and in most cases a green hard immature
37 fruit becomes more colourful, softer, sweeter and aromatic. Numerous physical and chemical
38 attributes that can be quantified during ripening include size, shape, texture, firmness, external colour,
39 internal colour, concentration of chlorophyll, soluble solids content (SSC), starch, sugars, acids, oils,
40 and internal ethylene concentration [1]. It is not realistic to assess simultaneously all the quality
41 attributes in the field with non-destructive methods and destructive laboratory measurements are
42 time-consuming due to the large number of samples required to take account of the within-field
43 variability [2]. Simple representative non-destructive measurements are thus required to assess the
44 ripeness of a fruit.

45 The measurement of fruit maturity in a non-destructive manner dates back more than half
46 century ago with the development of light transmittance techniques [3,4]. Since then a variety of
47 non-destructive techniques have been introduced including colorimetry [5], visible imaging [6],
48 visible and near infrared (VNIR) spectroscopy [7], hyperspectral imaging [8], multispectral imaging
49 [9], fluorescence imaging [10], acoustic impulse technique [11], Computed Tomography (CT) scan
50 [12], Magnetic resonance imaging (MRI) [13], acoustical vibration technique [14] and electronic nose
51 technique [15]. The first six techniques listed above will be considered in this review as they are the
52 most likely to be used in portable devices to enable pre-harvest in field assessment of fruit ripeness.
53 These techniques have been applied to studies of a large number fruits and external quality
54 attributes have been measured and correlated with internal characteristics, as shown in Table 1. The
55 non-destructive methods can produce a large amount of data with multiple variables and thus
56 multivariate analysis is utilized to identify key discriminatory variables that correlate with the
57 ripening status of a fruit [16]. Such key discriminatory variables can be used in regression models
58 enabling an assessment of fruit quality and thus ripeness.

59 Currently, the harvest time is mainly estimated by counting of days after flowering, subjective
60 tasting or visual assessment of fruit colour, texture or plant canopy structure [17,18]. All of these
61 methods on their own or in combination are time consuming and not necessarily accurate. The
62 quality attributes or the maturity indices derived from non-destructive techniques can however be
63 modelled to predict the optimal time of harvest. Such predictions need to account for changes in
64 environmental conditions and being a primary factor affecting the rate of plant development [19],
65 air temperature is a key parameter utilized in models predicting optimal harvest time [20]. An
66 example of a typical approach in developing a work flow for predicting optimal harvest date is
67 given in Figure 1.



68

69

Figure 1. A scheme of the overall workflow for the prediction of the optimal harvest date.

70 Here we review the non-destructive techniques for the fruit ripeness assessment and the
71 modelling for the prediction of an optimal harvest time. These predictions are based on imaging
72 and/or spectroscopic techniques that quantify the colour and/or spectral qualities of fruits that
73 change due to their molecular composition during the ripening process.

74

75
76
77

Table 1. Overview of the non-destructive methods for the assessment of fruit ripening. Abbreviation: SSC (Soluble solid content), DM (Dry matter), MC (Moisture content), TTA (Titratable acidity) and TSS (Total soluble solid)

	Colorimetry	Visible imaging	Spectroscopy	Fluorescence	HSI	MSI
Apple	Colour [21]	Colour [22]	Chlorophyll [23], anthocyanins [24], carotenoids [24], flavonols [25], SSC [26], firmness [27]	Chlorophyll [28], Anthocyanins [29], Flavonols [29], Firmness [29], SSC [29]	Firmness [30], SSC [31]	Firmness [32], SSC [33]
Pear			Firmness [34], SSC [35]		SSC [36]	
Peach	Colour [37]		Firmness [38], Chlorophyll [39], Colour [37]	Firmness [40]	Firmness [41]	Firmness [9], SSC
Avocado			MC [42], DM [42]		DM [43]	
Nectarine	Colour [44]		SSC [45], firmness [45]	Firmness [40]		
Mango	Colour [46]		DM [47], starch [48], SSC [47], colour [49], firmness [50]		Firmness [8], SSC [8], water content [8]	
Banana	Colour [51]	Colour [51]	TSS [52], Chlorophyll [53]		Firmness [54], TSS [54]	
Tomato	Colour [55], Firmness [56], TSS [57]	Colour [58], firmness [59]	Lycopene [60], SSC [61]	a*/b* [62]		Phenolic [63], lycopene [63]
Melon			SSC [64]			
Mandarin			TTA [65], SSC [66], firmness [67], DM [68]			
Cherry	Colour [69]		Firmness [70], SSC [71]			
Strawberry			Colour [72], TSS [73], Firmness [72], TTA [73]		Firmness [74], TSS [75], TTA [75]	SSC [76], firmness [77]
			SSC [78],			

Apricot			firmness [78], TTA [78]			
Kiwifruit			TSS [79], SSC[79], firmness [80], DM[81], Starch content [79]			
Persimmon			SSC [82]		Firmness [83]	
Grape			SSC [84], TTA [84], anthocyanin [85]	Chlorophyll [86], anthocyanin [86], TSS [86], flavonol [87]	SSC [88], TTA [88]	
Pineapple		Colour [89]	DM [90], SSC [91]			
plum			Firmness [92], SSC [93], colour [92]			

78 2. Colour measurement

79 The colour and appearance of a fruit is the initial quality assessment consumers use to judge
80 the acceptability of a fruit. These criteria are related to physical and chemical changes occurring
81 during fruit ripening [16,94]. In many fruits, during ripening colour change occurs due to
82 chlorophyll degradation and the increase in the concentration of pigments such as carotenoids or
83 polyphenols [95]. Several fruits have been studied for the relationship between maturity and colour
84 including tomato [96], orange [95], guava [97], peach [98], nectarine [99], mango [46,100], blueberry
85 [101], cherry [101] and pineapple [89]. To measure the changes in fruit colour the use of
86 colorimeters and image capture and analysis are the two major methods.

87 2.1. Colorimeter

88 Colorimeters are traditional non-destructive instruments used extensively in the fruit industry
89 to measure fruit colour [102]. They are more precise than human visual assessment and
90 standardization using CIELAB colour space, which was introduced by Commission Internationale
91 de l'Eclairage (CIE) in 1976, provides unified measurements [103]. The three coordinates of CIELAB
92 colour space, L^* , a^* and b^* , represent the respective values of lightness and the green to red and
93 blue to yellow ratios. CIELAB is close to human perception of colour due to the uniform
94 distribution of colours and all the colours can be perceived by human eye can be located on the
95 three coordinates [104]. Several colour indexes have been developed as the indicator of ripeness. In
96 certain experiments only the a^* parameter was correlated with colour change [97,103,105]. The b^*
97 value has only been reported to be positively correlated with ripeness in peach [37]. Using more
98 than one of the colour components improves the assessment of ripeness. The ripeness of tomato has
99 been assessed using the ratio between a^* and b^* and it showed high positive correlation with
100 lycopene concentration [106–108] and identifies significant differences for the six USDA ripening
101 classes [56,102]. Equations based on a^* and b^* include determining the hue angle and chroma. The
102 hue angle was found to be one of the best parameters to discriminate different ripeness stages for
103 tomato, peach and guava [37,97,102,106,108]. L^* value was also incorporated to the colour models
104 with a^* and b^* including citrus [109] and tomato [103]. Portable colourimeters are now available

105 commercially [46] and can be carried to the field. However, single fruit measurement limits its
106 application to map the ripeness of fruits in the whole field.

107 Data obtained with colourimeters has been successfully correlated with fruit ripeness thanks to
108 multivariate analyses. These statistical tests allow the simultaneous model with multiple variables
109 for example multiple linear regression (MLR) has been used to predict accurately the maturity of
110 mango using a^* b^* and their product as the variables [46]. Other regression methods were also
111 tested in this study including Partial Least Square (PLS) regression and Principal Component
112 Regression (PCR), but the prediction performance were slightly worse than MLR in the study by
113 Jha et al. [46].

114 2.2. Visible imaging

115 Colorimeters are not able to obtain representative colour values due to the limited sampling
116 area compared to the size of the fruit [110]. This limitation can be overcome by 2D colour imaging
117 that converts photons reflected from fruit skin to electrical signals and received by camera with
118 CCD (Charge-Coupled Device) or CMOS (Complementary Metal Oxide Semiconductor) sensors.
119 Normally, the sensor receives the light and filters it to three channels, which are R (red), G (green)
120 and B (blue) and the intensity values are always determined by fruit samples, illumination and the
121 internal characteristics of the camera [111].

122 Similar to $L^*a^*b^*$ colour space it is possible to analyze fruit ripeness in RGB colour space.
123 Schouten et al. showed that the R component can be used to describe the progressive colour change
124 of tomato at different stages of ripeness and correlates with changes in fruit firmness [59]. As
125 ripening is a continuously changing process the exact colour boundaries between different ripeness
126 stages are difficult to determine and if used arbitrary thresholds for each colour channel need to be
127 provided. Fuzzy logic, a statistical analysis approach reviewed by Yuan et al. [112], can overcome
128 the need for discrete thresholds and has been applied to the ripeness assessment of mango and
129 apple [22,113]. Goel et al. used the difference between R and B values to enhance the classification
130 of the different tomato ripeness stages reaching 94.3% accuracy [114].

131 Other statistical methods utilized includes unsupervised classification such as K-means and
132 Gustafson-Kessel algorithms, as reviewed in the study of Hartigan et al. and Lesot et al.
133 respectively [115,116]. These have successfully been applied to automatically separate banana of
134 different ripeness stages based on their RGB values [22]. Rather than only using the average RGB
135 values, the histogram of each channel was used to match with predefined reference histograms for
136 each ripeness group [22].

137 RGB values from images can be transformed to $L^*a^*b^*$ values and a comparable performance
138 was obtained with a colorimeter for the internal quality assessment of tomato fruits including Brix
139 and lycopene content [117]. Similar conclusion was drawn from studies in tomato [118], cherry [101]
140 and banana [94]. The RGB values are, however, device dependent and not a perceptually uniform
141 space, calibration is therefore crucial before the transformation of RGB values into $L^*a^*b^*$ space and
142 produce parameters comparable with a colorimeter [104]. Statistical modelling approaches
143 including quadratic and neural network models, as described in [119,120], were the best models to
144 convert RGB values into $L^*a^*b^*$ space [111] and Taghadomi et al. adopted the neural network
145 method and obtained a very strong correlation ($R^2=0.99$) between actual $L^*a^*b^*$ and RGB values in
146 cherry [101].

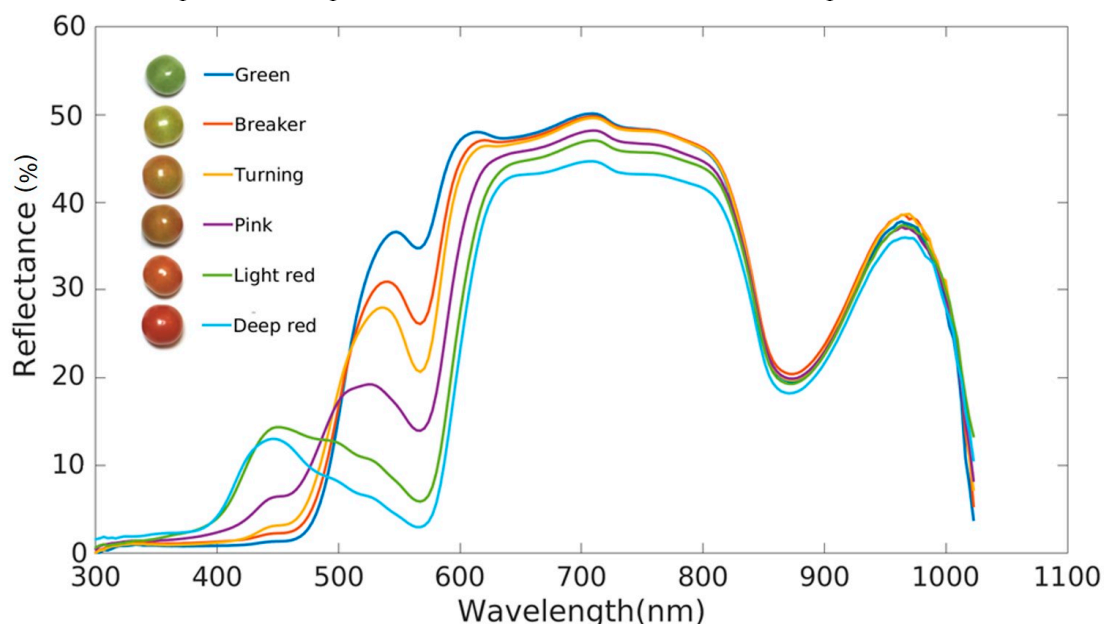
147 Other colour space values such as HSI (for Hue, Saturation and Intensity) and HSV (Hue,
148 Saturation and Value), can be derived from RGB values, can better represent human visual
149 perception [89]. Hue is defined as the similarity to the defined colours as red, green, blue and
150 yellow [121] and Saturation is used to describe how colourful a stimulus is relative to its own
151 brightness [122]. Fuzzy logic was successfully applied to group pineapple into three ripeness stages
152 using values derived from H, S and I [89]. Ukirade et al. used H, S and V values as the input of the
153 neural network model to classify tomato into four ripeness groups [123]. El-Bendary et al. proposed
154 a more sophisticated method for tomato, which used the colour histogram in HSV space and the
155 colour moments (mean, standard deviation and skewness) which measure the colour distribution in

156 an image as the colour features [124]. Principal Component Analysis (PCA) was applied to extract
 157 the features for both Linear Discriminant Analysis (LDA) and Support Vector Machine (SVM)
 158 models with more than 80% Correct Classification Rate (CCR) for five ripening stages [55]. Rather
 159 than only using one colour space, colour components from two colour spaces can be combined such
 160 as the study by Li et al, which used R, B and H from outdoor colour images of blueberry and it was
 161 found K-Nearest Neighbour (KNN), which classifies an object based on a majority vote among its
 162 neighbours [125] could achieve more than 85% CCR to separate four ripening stages [126].

163 Compared with a colourimeter, colour information can be obtained rapidly from larger area in
 164 a 2D image due to the high spatial resolution. The equipment can also be easily attached to moving
 165 platform such as tractor, robot or drone for rapid collection of multiple data collection
 166 measurements. There are however challenges that need to be overcome for 2D imaging including
 167 the difficulty of segmentation of fruits from background, device dependent RGB values and
 168 requirement of homogeneous illumination in the field.

169 3. Visible and infrared spectroscopy

170 When light hits the surface of a fruit it can be absorbed, scattered or re-emitted. The amount of
 171 each of these is determined by the physical properties and chemical constituents and thus ripeness
 172 of a fruit. Visible and Near InfraRed (VNIR) reflectance spectroscopy measures reflected light
 173 between 380 nm and 2500 nm, which is largely dependent on the light absorption by fruit sample
 174 and relates to almost all the major organic compounds. An example of the changes in spectra
 175 during ripening is given in Figure 2 that shows marked changes in the values between 400-700nm
 176 and also notable changes can be observed at longer wavelengths. VNIR spectroscopy has been
 177 widely applied as a non-destructive and fast measurement method for multiple quality attributes
 178 [127]. More importantly, a portable device has been developed and used in the field [128]. The
 179 recorded spectra can be analyzed and related to different ripeness stages by using spectral indices.
 180 The whole wavelength scan or values at key selected wavelengths are used in regression models to
 181 correlate with specific fruit qualities that that is associated with fruit ripeness.



182

183 **Figure 2.** Typical progressive change of reflectance spectra at different ripening stage of tomato and
 184 the legend showed corresponding colours

185 3.1. Spectral indices

186 Spectral indices normally combine the surface reflectance at two or more wavelengths to
 187 indicate relative abundance of a feature of interest as it is difficult to use only one wavelength as

188 indices for in-field assessment because the values can be highly affected by the sensor,
189 environmental illumination and particle size [129]. A number of spectral indices have been
190 calculated to describe the progressive change of peel pigment concentration during ripening. Ruiz-
191 Altisent et al. found that the reflectance at 450nm and 680nm were both associated with peach
192 firmness, but when using the reflectance values from only two wavelengths the linear correlation
193 factor was low ($R^2 < 0.6$) [130]. The index of absorption (I_{AD}) introduced by Ziosi et al., is a robust
194 spectral index obtained in calculating the difference between the absorption at two wavelengths
195 around the chlorophyll-a peak (670nm and 720nm) [131]. I_{AD} range was found to be similar across
196 different growing seasons and a good correlation with ripeness was found for peach [98,132],
197 apricot [133], nectarine [134,135] and plum [92]. Merzlyak et al. identified several spectral indices
198 for the quantification internal quality attributes of apple related to its ripeness with high correlation
199 ($R^2 > 0.8$) [24]. Zude et al. also developed three indices including the ratio between the transmission at
200 698nm and 760nm, NDVI and red-edge vegetation stress index (RVSI). Even though all these
201 indices showed good correlations with colour change of apple peel, the correlation appears to be
202 cultivar dependent as lower for the cultivar of 'Jonagold' than "Elstar" [23]. The same phenomenon
203 was also noticed in the study of Shinya et al. that the correlation between firmness and I_{AD} could be
204 extremely different among three cultivars of peach [98].

205 3.2. Full or selected wavelengths

206 Spectral indices can describe the change of peel pigment concentration during ripening process
207 and provide comparable values with the colorimetric method [37], but peel colour is not always the
208 only criteria for ripening assessment. The correlation between internal quality attributes related to
209 ripening such as firmness and SSC were investigated with full or selected wavelengths from VNIR
210 spectra.

211 For the full wavelengths, PLS is the most used regression model to predict fruit quality. The
212 prediction is achieved by extracting a set of orthogonal factors from the predictors called latent
213 variables which have the best predictive power [136]. Another common regression model is the
214 Principal Component Regression (PCR), which uses Multiple Linear Regression (MLR) to correlate
215 with the principal components scores extracted from the predictors [137], has been applied in some
216 studies for fruit quality assessment [138–140]. Compared with PLS, PCR showed the drawback that
217 the principal components were obtained without considering the dependent variables.

218 The variability of physical sample properties and/or the performance of the hardware can
219 result in undesired results including light scattering, path length variations and random noise
220 generated in the extracted spectra. These factors will reduce the accuracy and robustness of the
221 prediction models [141]. In order to improve the data analysis, a number of studies have applied
222 different pre-processing techniques to the spectra obtained before modelling [142].

223 Savitzky-Golay (SG) is the most frequently used digital data smoothing filter
224 [42,49,65,91,143,144], which applies linear least squares method to fit low-degree polynomial [145].
225 However, SG have contrasted effects on the performance of multivariate statistical models [146].
226 For example, Jha et al. compared different pre-processing techniques and found that smoothing did
227 not show any improvement in comparison with other techniques for the assessment of the firmness
228 in mango [49]. But Herrera et al. showed that SG filters using a second-order polynomial performed
229 better than other scattering correction methods for the prediction of wine grape brix [143]. Standard
230 Normal Variate (SNV) [72,78,147,148] and Multiple Scattering Correction (MSC)
231 [42,67,140,143,144,149] are the two most frequently used techniques for scattering correction. MSC
232 is used to eliminate the nonlinear scattering due to the non-uniform travel distance of light by
233 linearizing each spectrum to a reference spectrum, which is the always the mean spectrum [138].
234 Previous research has shown the similarity between SNV and MSC, for example Ma et al.
235 confirming the correlation coefficients were the same when assessing the sugar content of peach
236 using PLS models with SNV and MSC [150]. SNV can however be applied to individual spectrum
237 without requiring a reference [151]. In some studies, SNV was performed with de-trending, which
238 was used to correct the baseline shift of spectra [72,72,148].

239 Generating derivatives of spectra are useful pre-processing techniques to enhance subtle
240 differences and reduce the effect of specular reflection [79,143]. Guo et al. found that the PLS
241 regression model performed better with first derivative of the spectra than SNV, MSC, and the
242 second derivative for predicting the Soluble Solid Content (SSC) in strawberry [144]. A similar
243 conclusion was drawn for the Total Soluble Solid (TSS) content prediction of strawberry [73].
244 Second derivative has also been used in the prediction of chlorophyll content of apple [23], the SSC
245 of kiwifruit, strawberry, cherry, and peach [71,79,152,153], and the firmness of apricot [78]. Carlini
246 et al. compared the second derivative, MSC and SNV methods and found the second derivative
247 showed the best performance for the prediction of SSC of cherry [71]. Interestingly, pre-processing
248 techniques are not always beneficial to the spectral analysis. Clement et al. applied all mentioned
249 pre-processing techniques to the prediction of tomato ripeness, but it was found none of them
250 showed improvement on a PLS model due to the low levels of noise [154]. Likewise, Jaiswal et al.
251 also found that the best predictions of TSS and DM (Dry Matter) content of banana with PLS model
252 was obtained with no pre-processing to the spectra [52].

253 In some studies, only a small number of selected wavelengths were used to reduce the
254 multicollinearity among variables and modelled by Multiple Linear Regression (MLR) model. The
255 key wavelengths can be identified manually or automatically. The manual selection of key
256 wavelengths has been used for the prediction of brix of mango [155] and SSC for grape, lime and
257 star fruit [84]. Guthrie et al. calculated the correlation coefficients between second derivative of
258 spectra and brix values as the criteria of wavelength selection for MLR model. This method
259 provided better predictions than when using the first derivative [47] and had previously been used
260 in the prediction peach brix levels [156].

261 Automated wavelength selection method such as stepwise wavelength selection has also been
262 used to aid the predictive power of models. The first wavelength is selected with the highest
263 correlation to the dependent variable, and for each step the candidate wavelength was added to
264 increase the correlation until none of the remaining wavelengths were significant. This method was
265 used for the SSC prediction of peach [157], melon and pineapple [158]. Genetic Algorithm (GA),
266 which uses natural selection and random mutations based on prediction accuracy is another
267 efficient automated method in identifying key wavelengths and was successfully applied to SSC
268 prediction of apple [159].

269 A comparison of the performance of PLS and MLR for the assessment of maturity of mango
270 indicated that when using MLR, poorer correlation of data was observed and led to overfitting as
271 seen by the large gap between the correlation coefficients of calibration and validation models [160].
272 Similar phenomenon was also observed for the prediction of TSS and DM for banana [52].
273 However, if the key wavelengths were selected with most of the variance of the whole spectra but
274 low collinearity, MLR can show better performance than PLS such as the firmness prediction of
275 mango [50]. These two methods of modelling were also compared for the prediction of brix value of
276 mango and interestingly both correlation coefficients were high and comparable [155].
277 Consequently, it is unclear which model can provide better prediction as the performance of MLR is
278 largely dependent on the wavelength selection.

279 The correlation was always higher for the prediction of SSC than firmness of fruit by using
280 spectroscopic methods. Park et al. showed that the prediction of firmness was more complicated
281 than SSC as it was not determined by a single analyte or a limited group of related chemicals [139].
282 For both SSC and firmness prediction, the performance of the model is always cultivar dependent,
283 and the calibration model trained by using mixed cultivars produces lower correlation than when
284 using results from an individual cultivar. Limited number of studies were focused on the
285 assessment in field, but compared with indoor measurement, the prediction is less accurate
286 [27,45,48].

287 Similarly with colourimeter, spectroscopy is not likely to be applied as high-throughput
288 ripening assessment due to the low spatial resolution. The accuracy of the internal quality
289 measurement is influenced by sample temperature, which needs to be compensated by an extra
290 calibration model [48]. Spectroscopy has been used in assessing the quality of a large variety of

291 fruits and portable commercial spectrometers have been developed [48,78,128,161] but most of the
292 studies focused on indoor post-harvest assessment of fruit maturity. Inconsistent performances
293 were observed for the models developed by spectra taken indoor and on-tree. Predicting apple
294 firmness and SSC both on the tree and during storage showed that 'on tree' PLS model had the best
295 correlation coefficients for both firmness and SSC [27,162]. However, for nectarine, the 'on tree'
296 model performed worse than post-harvest [45]. Consequently, for the on-tree ripeness assessment,
297 it is necessary to build the prediction model with spectra taken in-field and understand the effect of
298 environmental factors on the quality of spectra.

299 4. Fluorescence

300 Fruit degreening i.e. the loss of chlorophyll is an effective indicator of fruit ripening and thus
301 measuring chlorophyll content using a fluorimetric sensor can be correlated to fruit ripeness traits
302 [163].

303 One chlorophyll fluorimetric method measures the photochemical and non-photochemical
304 processes with the illumination of actinic light [164]. A Pulse-Amplitude-Modulation (PAM) based
305 fluorometer has been developed commercially, which uses visible light at blue region as the
306 excitation and measures minimum (F_0) and maximum (F_m) emitted fluorescence. The maximum
307 quantum yield $(F_m - F_0)/F_m$ was calculated and this parameter was found to be negatively correlated
308 with the ripening stage of apple [165] and papaya fruit [166]. This chlorophyll fluorimetric method
309 is popular in the laboratory, but difficult to be applied in field as the samples need to be dark-
310 adapted. For example, the papaya samples in the study of Urbano et al. were dark-adapted for 30
311 mins with a dark towel [166]. Bodria et al. designed a fluorescence imaging system which measured
312 the light emission at 690 - 740 nm with the excitation light in UV-blue and red regions, and good
313 correlation was achieved between the quality parameters including firmness and SSC of fresh apple
314 and detected fluorescence even though hue value of skin colour showed little change, but for peach
315 and nectarine, the correlation was lower [163]. The fruit samples measured by this fluorescence
316 imaging system were not dark adapted, but the equipment has only been designed for the
317 laboratory use.

318 In order to reduce the influence of the environmental factors on the absolute fluorescence
319 intensity at single band, which limits in-field application [167], more studies were focused on the
320 understanding of the fluorescence ratios using various light sources of defined wavelengths, which
321 has led to the development of a handheld multi-parametric fluorescence sensor – Multiplex®
322 (Force-A, Orsay, France) with four LED light sources and three synchronized fluorescence detectors
323 [10]. The most common informative indices utilized fluorescence from anthocyanins (ANTH),
324 flavonols (FLAV), and chlorophyll (CHL) to indicate fruit ripeness. In the study of Betemps et al.,
325 CHL showed positive correlation with the firmness of apple and they also obtained good negative
326 correlation between FR_RED and SSC [29]. In field assessment of CHL was also successfully
327 applied to grape with a high correlation with TSS and the combination of CHL and ANTH can be
328 used as a robust decision tool to predict harvest time [86]. For tomato, all the indices were found to
329 correlate well with the time-shift in the tomato ripening process in the study of Hoffmann et al. [62].
330 The blue to red fluorescence ratio (B_UV/RF_UV) was measured as an effective parameter for the
331 assessment of the ripeness of oil palm with rough skin, and with the Classification and Regression
332 Tree (C&RT) method resulting in an overall correct classification rate of 90% for three different
333 ripeness stages [168].

334 5. Spectral imaging

335 5.1. Hyperspectral imaging (HSI)

336 Hyperspectral imaging (HSI) has emerged as a powerful tool for the inspection of fruit quality.
337 HSI generates a three-dimension imaging cube with images at a range of continuous wavelengths.
338 A single spectrum can be extracted from each individual pixel representing the absorption
339 properties and the textural information of fruit samples [169]. Similar with traditional visible

340 imaging and spectroscopic methods, HSI is non-destructive and requires little sample preparation,
341 but it is advantageous that it can record both spatial and spectral information simultaneously [170].
342 For the assessment of fruit quality, two types of wavelength dispersion devices are normally used
343 i.e. line scanning and area scanning coupled with an imaging sensor for the HSI image acquisition.
344 A line scanning device has the imaging spectrograph dispersing the incident light into different
345 wavelengths instantaneously between visible and near infrared wavelength range (380-1700 nm).
346 Line scanning HSI cameras scan the samples continuously in one direction, so they can be attached
347 to moving platforms such as tractors [171], robots [172] and unmanned aerial vehicles (UAV) [173].

348 The hyperspectral image can be handled in two different ways 1) light scattering analysis and
349 2) spectral analysis. Modified Lorentzian Distribution (MLD), that correlates the data obtained with
350 a predefined distribution curve by using a distribution function, can be used to describe the
351 scattering profile and the fitting parameters were used as the variables of stepwise MLR model [30].
352 The results of this study suggest that spectral scattering from all wavelengths or selected
353 wavelengths can provide more accurate prediction of apple firmness than using the secondary
354 properties such as spectral absorption [30]. Similar methods were also employed for the prediction
355 of peach firmness, but with MLR models different results were obtained when using two different
356 cultivars [41]. Mendoza et al. combined both the spectral and image analysis techniques on
357 scattering images including discrete and continuous wavelet transformation decomposition, first
358 order statistics, Fourier analysis, co-occurrence matrix, and Variogram analysis but little
359 improvement on the prediction of firmness and SSC of apple was found, with the performance of
360 PLS model being cultivar dependent [174]. Wang et al. used two different feature selections
361 methods which were Uninformative Variable Elimination (UVE) [175] and Supervised Affinity
362 Propagation (SAP) [176]. The output of two PLS models with two feature selection methods were
363 combined as the input into an ANN model that gave a correlation coefficient of 0.83 [177]. The
364 scattering profile was also used for the prediction of firmness of peach [41].

365 The average spectra of the region of interest (ROI) have also been modelled for the assessment
366 of fruit quality. The average spectra from whole wavelength scan (400-1000 nm) were used with a
367 PLS model to predict the SSC of grape and the correlation coefficients were similar for both white
368 and red grape [88]. The same method has also been used to predict the TSS of strawberry [178] and
369 the firmness and SSC of blueberry [179]. Key wavelengths have also been selected before modelling
370 in order to reduce the redundancy of the whole spectral dataset with different feature selection
371 techniques. One of widely used feature selection criteria is based on beta coefficients derived from
372 PLS model, which measured how great effect an independent variable have on the dependent
373 variable. A comparison of the performance between the MLR models with selected wavelengths
374 based on beta coefficients and PLS model with full spectra as input, showed that the final outcomes
375 were similar for the internal quality measurement of strawberry [178]. The same feature selection
376 methods were also used by Rajkumar et al. to predict the firmness and TSS of banana by MLR
377 model, and good correlation was achieved for both quality attributes with correlation coefficients of
378 0.91 and 0.85 [54]. Another key wavelength selection method to solve collinearity problem is the
379 Successive Projection Algorithm (SPA), which iteratively adds one wavelength until a specific
380 number of wavelength was achieved with minimum redundant information content [180], has been
381 used to select the feature wavelengths as the input of PLS model and high correlation ($R^2 = 0.92$)
382 was found for predicting persimmon firmness [83].

383 Overall HSI is a promising technique for fruit ripeness assessment. In-field application of this
384 technique will need to overcome the challenges of handling the large data output and the
385 calibration of variable light levels whilst in the crop.

386 5.2. Multispectral imaging (MSI)

387 Multispectral imaging (MSI) is a form of HSI that collects data at specific wavelengths instead
388 of scanning the whole wavelength range. This can be accomplished using a frame scanning imaging
389 system with Liquid Crystal Tunable Filter LCTF coupled with CCD (charge-coupled device) or
390 CMOS (complementary metal oxide semiconductor) sensor. Lu et al. used five wavelengths based

391 on previous studies to correlate their scattering profiles with the firmness and SSC of apple using
392 an ANN model and obtained reasonably high correlation for both quality attributes, which were r^2
393 = 0.87 and 0.77 respectively [181]. Another lower-cost MSI system uses a rotating filter wheel
394 containing a few bandpass filters instead of LCTF, but the tuning speed is lower than LCTF. This
395 device has been used to predict the firmness and SSC of peach with the best combination of four
396 wavelengths and high correlation coefficients were achieved as 0.94 and 0.97 respectively [76]. The
397 prediction of firmness was higher than the prediction by HSI [41]. Similarly, Liu et al. used MSI
398 with 19 wavelengths to predict the firmness and TSS of strawberry, and PLS, SVM and ANN were
399 compared with the best correlation coefficient of 0.94 and 0.83 respectively [74], which was
400 comparable with HSI for prediction of TSS of strawberry [178].

401 Compared with HSI, MSI can be lower cost and easier to convert into portable device and the
402 output imaging dataset will be smaller. A portable MSI device with four narrow-band light sources
403 and four reflectance sensors of different wavelengths at 570, 670, 750 and 870nm has been
404 developed [130]. This device was used to classify oil palm into different stages of ripeness using
405 quadratic discriminant analysis and discriminant analysis with Mahalanobis distance classifiers
406 with a >85% of correct classification rate being achieved [182].

407 6. Prediction of optimal harvest date

408 Non-destructive methods are very promising for the ripeness assessment in field, but the most
409 critical question is to how to link such assessment to predict yield and the optimal harvest date and
410 [18]. This is highly challenging and made complicated by ripeness variability within and between
411 plants.

412 Yang et al. recorded the HSI spectra of tomatoes at different growing stages and PLS model
413 was applied to predict the growing stage with the best correlation coefficient of 0.89. It was also
414 found that the key wavelengths were in the visible and infrared regions (400-2100 nm) [183]. A
415 Similar method was employed to predict the number of days before commercial harvest of apple.
416 The calibration model was built with eight cultivars and good correlation ($R^2=0.93$) was found for
417 the spectral range between 380 nm and 2000 nm [184]. Environmental factors such as temperature,
418 light levels, humidity, etc. significantly influence the development of crop fruit, and it is essential to
419 incorporate important environmental factors predictions for the determination of the optimal
420 harvest date [185]. Several crop models have been developed since the 1960s by Loomis et al. [186]
421 with the input of environmental factors both for in-field and greenhouse prediction. Such models
422 are difficult to use due to the number of input variables [187–192]. Qiu et al. investigated the
423 dominant environmental factors in greenhouse for tomato growth and it was found that
424 temperature, humidity and photosynthesis active radiation (PAR) show positive or negative
425 correlation to crop growth [192]. The influence of temperature has also been reported in a number
426 studies such as for tomato [185], grape [193], apple [194], mango [195], blueberry [18], apricot [196]
427 and strawberry [197]. Shewfelt et al. studied the colour change at different constant temperatures,
428 but the variation of the temperature within each day was not considered [96]. Munoz et al.
429 developed a time series regression model for the prediction of harvest date of blueberry, and the
430 minimum and maximum of daily temperature from weather forecast from two weeks ahead were
431 used as the input the model [18]. This method was closer to real application and potentially could
432 be applied with non-destructive techniques, which could determine the current ripening stage.
433 Environmental temperature affected the fruit growth, and it was also found the fruit temperature
434 also influenced the near infrared reflectance spectrum in a non-linear way [146]. Kawano et al.
435 compensated the surface temperature effect by developing combined MLR model which covered a
436 variation of temperature ranged between 21 to 31 °C [198]. Peirs et al. compared global calibration
437 model that covers a wide temperature range and calibration models for each temperature range and
438 both methods performed well for the SSC prediction of apple, but for the practical purpose, global
439 calibration model was preferred [26].
440

441 7. Conclusions

442 Although now becoming slightly outdated the key study by the Food and Agricultural
443 Organisation (FAO) indicated that global food waste and losses in 2009 was estimated to be one-
444 third (by weight) of all food produced in the world [199]. The prevention of such losses and waste is
445 therefore a major driver to improve global food security. Here we have reviewed a range of non-
446 destructive techniques and the data modelling methods for the assessment of fruit ripening and the
447 prediction of optimal harvest date. Knowing when to pick will not only depend on the fruit to
448 ensure the optimal taste, quality and postharvest performance but also on the local circumstances
449 including, weather, the supply chain and markets. Having an affordable portable device to inform
450 this decision is crucial and the non-destructive techniques discussed above have all been developed
451 into such devices that will greatly help to reduce waste.

452 Such devices include colourimeters that can record accurate colour information but only for
453 individual fruit. 2D imaging overcomes this limit as it images larger area and can be fitted on
454 moving platform, but 2D imaging can only obtain colour information which is not adequate as the
455 indicator of ripeness for all fruits. Similar with colourimeter and 2D imaging, fluorescence detect
456 the colour change especially the change of content of chlorophyll. Spectroscopy in visible and NIR
457 region correlates with both colour and internal quality attributes, which can provide better
458 prediction of fruit ripeness. Hyperspectral imaging has the advantage of both spectroscopy and 2D
459 imaging and can be integrated with moving platform, but due to the high expense and large dataset
460 generation, it is still mainly used in the lab. Multispectral imaging has the potential to overcome the
461 limitation of hyperspectral imaging but the reliability of the measurement in field needs to be
462 further investigated. The miniaturization and computational capacity will be a major technical
463 hurdle in ensuring that the devices can be used in the field and provide real time assessment of fruit
464 quality and ripeness. Simultaneous to the development of the hardware the data modelling
465 techniques need to be implemented that can utilize not only data from the controlled laboratory
466 conditions but that from the more challenging field conditions, with the changeable environment.
467 **Author Contributions:** Dr. Bo Li is the key author, who reviewed previous literature and wrote the
468 manuscript; Dr. Julien Lecourt supervised the work, provided ideas and contribute to writing; Prof.
469 Gerard Bishop proposed the topic, supervised the work, contribute to writing and edit the
470 manuscript before submission.

471 **Conflicts of Interest** The authors declare no conflict of interest.

472 References

- 473 1. Cantwell, M. Maturation and Maturity Indices Quality. **2009**, 1–21.
- 474 2. Maristella Vanoli, M. B. Overview of the methods for assessing harvest maturity. *Stewart Postharvest Rev.*
475 **2012**, *8*, 1–6, doi:10.2212/spr.2012.1.4.
- 476 3. Birth, G. S.; Norris, K. H. An instrument using light transmittance for nondestructive measurement of
477 fruit maturity. *Food Technol.* **1958**, *12(11)*, 592–595.
- 478 4. Ernest, J. V.; Birth, G. A.; Sidwell, A. P.; Golumbic, C. Evaluation of light transmittance techniques for
479 maturity measurements of the purple plum (Italian prune). *Food Technology.* **1958**, *12(5)*, 42
- 480 5. Baltazar, A.; Aranda, J. I.; González-Aguilar, G. Bayesian classification of ripening stages of tomato fruit
481 using acoustic impact and colorimeter sensor data. *Comput. Electron. Agric.* **2008**, *60*, 113–121,
482 doi:10.1016/j.compag.2007.07.005.
- 483 6. Choi, K.; Lee, G.; Han, Y. J.; Bunn, J. M. Tomato Maturity Evaluation Using Color Image Analysis 1995,
484 38.
- 485 7. Yang, H. Q. Nondestructive Prediction of Optimal Harvest Time of Cherry Tomatoes Using VIS-NIR
486 Spectroscopy and PLSR Calibration. *Adv. Eng. Forum* **2011**, *1*, 92–96,
487 doi:10.4028/www.scientific.net/AEF.1.92.
- 488 8. Sivakumar, S. S.; Qiao, J.; Wang, N.; Gariépy, Y.; Raghavan, G. S. V; McGill, J. Detecting Maturity
489 Parameters of Mango Using Hyperspectral Imaging Technique 2006.

- 490 9. Lleo, L.; Barreiro, P.; Ruiz-Altisent, M.; Herrero, A. Multispectral images of peach related to firmness and
491 maturity at harvest. *J. Food Eng.* **2009**, *93*, 229–235, doi:10.1016/j.jfoodeng.2009.01.028.
- 492 10. Cerovic, Zoran G, Jean-Pascal Goutouly, Ghislaine Hilbert, Agnes Destrac-Irvine, Vincent Martinon, N.
493 M. Mapping winegrape quality attributes using portable fluorescence-based sensors Zoran. *8. Fruit, nut*
494 *Veg. Prod. Eng. Symp. FRUTIC 09* **2009**, 301–310, doi:10.3390/s101110040.
- 495 11. Stone, M. L.; Armstrong, P. R.; Zhang, X.; Brusewitz, G. H.; Chen, D. D. Watermelon maturity
496 determination in the field using acoustic impulse impedance techniques. *Trans. ASAE* **1996**, *39*, 2325–
497 2330, doi:10.13031/2013.27743.
- 498 12. Kotwaliwale, N. Monitoring of mango (*Mangifera indica* L.) (Cv.: Chousa) ripening using X-ray
499 computed tomography. *Ieee* **2012**, 326–330.
- 500 13. Zhang, L.; McCarthy, M. J. Measurement and evaluation of tomato maturity using magnetic resonance
501 imaging. *Postharvest Biol. Technol.* **2012**, *67*, 37–43, doi:10.1016/j.postharvbio.2011.12.004.
- 502 14. Taniwaki, M.; Hanada, T.; Tohro, M.; Sakurai, N. Non-destructive determination of the optimum eating
503 ripeness of pears and their texture measurements using acoustical vibration techniques. *Postharvest Biol.*
504 *Technol.* **2009**, *51*, 305–310, doi:10.1016/j.postharvbio.2008.08.004.
- 505 15. Brezmes, J.; Fructuoso, M. L. L.; Llobet, E.; Vilanova, X.; Recasens, I.; Orts, J.; Saiz, G.; Correig, X.
506 Evaluation of an electronic nose to assess fruit ripeness. *IEEE Sens. J.* **2005**, *5*, 97–108.
- 507 16. Wu, D.; Sun, D.-W. Advanced applications of hyperspectral imaging technology for food quality and
508 safety analysis and assessment: A review – Part I: Fundamentals. *Innov. Food Sci. Emerg. Technol.* **2013**,
509 *19*, 1–14, doi:10.1016/j.ifset.2013.04.014.
- 510 17. François, I. M.; Mariën, E.; Brijs, K.; Coppin, P.; De Proft, M. The use of Vis/NIR spectroscopy to predict
511 the optimal root harvesting date of chicory (*Cichorium intybus* L.). *Postharvest Biol. Technol.* **2009**, *53*, 77–
512 83, doi:10.1016/j.postharvbio.2009.03.003.
- 513 18. Muñoz, C.; Ávila, J.; Salvo, S.; Huircán, J. I. Prediction of harvest start date in highbush blueberry using
514 time series regression models with correlated errors. *Sci. Hort. (Amsterdam)*. **2012**, *138*, 165–170,
515 doi:10.1016/j.scienta.2012.02.023.
- 516 19. Hatfield, J. L.; Prueger, J. H. Temperature extremes: Effect on plant growth and development. *Weather*
517 *Clim. Extrem.* **2015**, *10*, 4–10, doi:10.1016/j.wace.2015.08.001.
- 518 20. Adams, S. R.; Cockshull, K. E.; Cave, C. R. J. Effect of temperature on the growth and development of
519 tomato fruits. *Ann. Bot.* **2001**, *88*, 869–877, doi:10.1006/anbo.2001.1524.
- 520 21. Ferre, G.; Massol, G.; Le Fur, G.; Villeneuve, F. Apple colour and ripeness. Use of a colorimeter: prospects.
521 *Infos CTIFL (France)* **1987**.
- 522 22. Dadwal, M.; Banga, V. K. Estimate Ripeness Level of fruits Using RGB Color Space and Fuzzy Logic
523 Technique. *Int. J. Eng. Adv. Technol.* **2012**, *2*, 225–229.
- 524 23. Zude, M. Comparison of indices and multivariate models to non-destructively predict the fruit
525 chlorophyll by means of visible spectrometry in apple fruit. *Anal. Chim. Acta* **2003**, *481*, 119–126,
526 doi:10.1016/S0003-2670(03)00070-9.
- 527 24. Merzlyak, M. N.; Solovchenko, A. E.; Gitelson, A. A. Reflectance spectral features and non-destructive
528 estimation of chlorophyll, carotenoid and anthocyanin content in apple fruit. *Postharvest Biol. Technol.*
529 **2003**, *27*, 197–211, doi:10.1016/S0925-5214(02)00066-2.
- 530 25. Solovchenko, A. E.; Chivkunova, O. B.; Gitelson, A. A.; Merzlyak, M. N. Non-Destructive Estimation
531 Pigment Content, Ripening, Quality and Damage in Apple Fruit with Spectral Reflectance in the Visible
532 Range. *Fresh Prod.* **2010**, 91–102.
- 533 26. Peirs, A.; Scheerlinck, N.; Nicolai, B. M. Temperature compensation for near infrared reflectance
534 measurement of apple fruit soluble solids contents. **2003**, *30*, 233–248, doi:10.1016/S0925-5214(03)00118-2.
- 535 27. Zude, M.; Herold, B.; Roger, J. M.; Bellon-Maurel, V.; Landahl, S. Non-destructive tests on the prediction
536 of apple fruit flesh firmness and soluble solids content on tree and in shelf life. *J. Food Eng.* **2006**, *77*, 254–
537 260, doi:10.1016/j.jfoodeng.2005.06.027.
- 538 28. Zude-Sasse, M.; Truppel, I.; Herold, B. An approach to non-destructive apple fruit chlorophyll
539 determination. *Postharvest Biol. Technol.* **2002**, *25*, 123–133, doi:10.1016/S0925-5214(01)00173-9.
- 540 29. Betemps, D. L.; Fachinello, J. C.; Galarça, S. P.; Portela, N. M.; Remorini, D.; Massai, R.; Agati, G. Non-
541 destructive evaluation of ripening and quality traits in apples using a multiparametric fluorescence
542 sensor. *J. Sci. Food Agric.* **2012**, *92*, 1855–1864, doi:10.1002/jsfa.5552.
- 543 30. Peng, Y.; Lu, R. Analysis of spatially resolved hyperspectral scattering images for assessing apple fruit

- 544 firmness and soluble solids content. *Postharvest Biol. Technol.* **2008**, *48*, 52–62,
545 doi:10.1016/j.postharvbio.2007.09.019.
- 546 31. Mendoza, F.; Lu, R.; Ariana, D.; Cen, H.; Bailey, B. Integrated spectral and image analysis of
547 hyperspectral scattering data for prediction of apple fruit firmness and soluble solids content. *Postharvest*
548 *Biol. Technol.* **2011**, *62*, 149–160, doi:10.1016/j.postharvbio.2011.05.009.
- 549 32. Peng, Y.; Lu, R. An LCTF-based multispectral imaging system for estimation of apple fruit firmness: Part
550 II. Selection of optimal wavelengths and development of prediction models. *Trans. ASABE* **2006**, *49*, 269–
551 275, doi:10.13031/2013.20224.
- 552 33. Peng, Y.; Lu, R. Prediction of apple fruit firmness and soluble solids content using characteristics of
553 multispectral scattering images. *J. Food Eng.* **2007**, *82*, 142–152, doi:10.1016/j.jfoodeng.2006.12.027.
- 554 34. Cavaco, A. M.; Pinto, P.; Antunes, M. D.; Silva, J. M. da; Guerra, R. “Rocha” pear firmness predicted by a
555 Vis/NIR segmented model. *Postharvest Biol. Technol.* **2009**, *51*, 311–319,
556 doi:10.1016/j.postharvbio.2008.08.013.
- 557 35. Shao, Y.; Bao, Y.; He, Y. Visible/Near-Infrared Spectra for Linear and Nonlinear Calibrations: A Case to
558 Predict Soluble Solids Contents and pH Value in Peach. *Food Bioprocess Technol.* **2011**, *4*, 1376–1383,
559 doi:10.1007/s11947-009-0227-6.
- 560 36. Tiansheng, H.; Jun, Q.; Wang, N.; Ngadi, M. O.; Zuoxi, Z.; Zhen, L. Non-destructive inspection of Chinese
561 pear quality based on hyperspectral imaging technique. *Trans. Chinese Soc. Agric. Eng.* **2007**, *2*, 29.
- 562 37. Ferrer, A.; Remon, S.; Negueruela, A. I.; Oria, R. Changes during the ripening of the very late season
563 Spanish peach cultivar Calanda: Feasibility of using CIELAB coordinates as maturity indices. *Sci. Hortic.*
564 *(Amsterdam)*. **2005**, *105*, 435–446, doi:10.1016/j.scienta.2005.02.002.
- 565 38. Lammertyn, J.; Nicolai, B.; Ooms, K.; De Smedt, V.; De Baerdemaeker, J. Non-destructive measurement of
566 acidity, soluble solids, and firmness of Jonagold apples using NIR-spectroscopy. *Trans. ASAE* **1998**, *41*,
567 1089.
- 568 39. Ziosi, V.; Noferini, M.; Fiori, G.; Tadiello, A.; Trainotti, L.; Casadoro, G.; Costa, G. A new index based on
569 vis spectroscopy to characterize the progression of ripening in peach fruit. *Postharvest Biol. Technol.* **2008**,
570 *49*, 319–329, doi:10.1016/j.postharvbio.2008.01.017.
- 571 40. Bodria, L.; Fiala, M.; Guidetti, R.; Oberti, R. Optical techniques to estimate the ripeness of red-pigmented
572 fruits. *Trans. ASAE* **2004**, *47*, 815–820, doi:10.13031/2013.16077.
- 573 41. Lu, R.; Peng, Y. Hyperspectral Scattering for assessing Peach Fruit Firmness. *Biosyst. Eng.* **2006**, *93*, 161–
574 171, doi:10.1016/j.biosystemseng.2005.11.004.
- 575 42. Olarewaju, O. O.; Bertling, I.; Magwaza, L. S. Non-destructive evaluation of avocado fruit maturity using
576 near infrared spectroscopy and PLS regression models. *Sci. Hortic. (Amsterdam)*. **2016**, *199*, 229–236,
577 doi:10.1016/j.scienta.2015.12.047.
- 578 43. Salazar-garcia, S. Evaluating Hass Avocado Maturity Using Hyperspectral Imaging. **2008**.
- 579 44. Luchsinger, L. E.; Walsh, C. S. Development of an objective and non-destructive harvest maturity index
580 for peaches and nectarines. In *Acta Horticulturae*; International Society for Horticultural Science (ISHS),
581 Leuven, Belgium, 1998; pp. 679–688.
- 582 45. Pérez-Marín, D.; Sánchez, M. T.; Paz, P.; Soriano, M. A.; Guerrero, J. E.; Garrido-Varo, A. Non-destructive
583 determination of quality parameters in nectarines during on-tree ripening and postharvest storage.
584 *Postharvest Biol. Technol.* **2009**, *52*, 180–188, doi:10.1016/j.postharvbio.2008.10.005.
- 585 46. Jha, S. N.; Chopra, S.; Kingsly, A. R. P. Modeling of color values for nondestructive evaluation of maturity
586 of mango. *J. Food Eng.* **2007**, *78*, 22–26, doi:10.1016/j.jfoodeng.2005.08.048.
- 587 47. Guthrie, J.; Walsh, K. Non-invasive assessment of pineapple and mango fruit quality using near infra-
588 red spectrometry. *Aust. J. Exp. Agric.* **1997**, *37*, 253–263, doi:10.1071/EA97144.
- 589 48. Saranwong, S.; Sornsrivichai, J.; Kawano, S. On-tree evaluation of harvesting quality of mango fruit using
590 a hand-held NIR instrument. *J. Near Infrared Spectrosc.* **2003**, *11*, 283–293, doi:10.1255/jnirs.374.
- 591 49. Jha, S. N.; Kingsly, A. R. P.; Chopra, S. Non-destructive Determination of Firmness and Yellowness of
592 Mango during Growth and Storage using Visual Spectroscopy. *Biosyst. Eng.* **2006**, *94*, 397–402,
593 doi:10.1016/j.biosystemseng.2006.03.009.
- 594 50. Schmilovitch, Z.; Mizrach, A.; Hoffman, A.; Egozi, H.; Fuchs, Y. Determination of mango physiological
595 indices by near-infrared spectrometry. *Postharvest Biol. Technol.* **2000**, *19*, 245–252, doi:10.1016/S0925-
596 5214(00)00102-2.
- 597 51. Mendoza, F. and Aguilera, J. M. Application of Image Analysis for Classification of Ripening Bananas.

- 598 *Food Eng. Phys. Prop. Appl.* **2004**, *69*, 478–487.
- 599 52. Jaiswal, P.; Jha, S. N.; Bharadwaj, R. Non-destructive prediction of quality of intact banana using
600 spectroscopy. *Sci. Hortic. (Amsterdam)*. **2012**, *135*, 14–22, doi:10.1016/j.scienta.2011.11.021.
- 601 53. Adebayo, S. E.; Hashim, N.; Abdan, K.; Hanafi, M.; Mollazade, K. Prediction of quality attributes and
602 ripeness classification of bananas using optical properties. *Sci. Hortic. (Amsterdam)*. **2016**, *212*, 171–182,
603 doi:10.1016/j.scienta.2016.09.045.
- 604 54. Rajkumar, P.; Wang, N.; Elmasry, G.; Raghavan, G. S. V.; Garipey, Y. Studies on banana fruit quality and
605 maturity stages using hyperspectral imaging. *J. Food Eng.* **2012**, *108*, 194–200,
606 doi:10.1016/j.jfoodeng.2011.05.002.
- 607 55. El-Bendary, N.; El Hariri, E.; Hassanien, A. E.; Badr, A. Using machine learning techniques for evaluating
608 tomato ripeness. *Expert Syst. Appl.* **2015**, *42*, 1892–1905, doi:10.1016/j.eswa.2014.09.057.
- 609 56. Batu, A. Determination of acceptable firmness and colour values of tomatoes. *J. Food Eng.* **2004**, *61*, 471–
610 475, doi:10.1016/S0260-8774(03)00141-9.
- 611 57. Saad, A.; Ibrahim, A.; El-Biale, N. Internal quality assessment of tomato fruits using image color
612 analysis. *Agric. Eng. Int. CIGR J.* **2016**, *18*, 339–352.
- 613 58. Gastélum-Barrios, A.; López-Bórquez, R.; Rico-García, E.; Toledano-Ayala, M.; Soto-Zarazúa, G. Tomato
614 quality evaluation with image processing: A review. *African J. Agric. Res.* **2011**, *6*, 3333–3339,
615 doi:10.5897/AJAR11.108.
- 616 59. Schouten, R. E.; Huijben, T. P. M.; Tijssens, L. M. M.; van Kooten, O. Modelling quality attributes of truss
617 tomatoes: Linking colour and firmness maturity. *Postharvest Biol. Technol.* **2007**, *45*, 298–306,
618 doi:10.1016/j.postharvbio.2007.03.011.
- 619 60. Clément, A.; Dorais, M.; Vernon, M. Nondestructive measurement of fresh tomato lycopene content and
620 other physicochemical characteristics using visible NIR spectroscopy. *J. Agric. Food Chem.* **2008**, *56*, 9813–
621 9818, doi:10.1021/jf801299r.
- 622 61. Clément, A.; Dorais, M.; Vernon, M. Multivariate approach to the measurement of tomato maturity and
623 gustatory attributes and their rapid assessment by Vis-NIR spectroscopy. *J. Agric. Food Chem.* **2008**, *56*,
624 1538–1544, doi:10.1021/jf072182n.
- 625 62. Hoffmann, A. M.; Noga, G.; Hunsche, M. Fluorescence indices for monitoring the ripening of tomatoes in
626 pre- and postharvest phases. *Sci. Hortic. (Amsterdam)*. **2015**, *191*, 74–81, doi:10.1016/j.scienta.2015.05.001.
- 627 63. Liu, C.; Liu, W.; Chen, W.; Yang, J.; Zheng, L. Feasibility in multispectral imaging for predicting the
628 content of bioactive compounds in intact tomato fruit. *Food Chem.* **2015**, *173*, 482–488,
629 doi:10.1016/j.foodchem.2014.10.052.
- 630 64. Long, R. L.; Walsh, K. B. Limitations to the measurement of intact melon total soluble solids using near
631 infrared spectroscopy. *Aust. J. Agric. Res.* **2006**, *57*, 403–410.
- 632 65. McGlone, V. A.; Fraser, D. G.; Jordan, R. B.; Künnemeyer, R. Internal quality assessment of mandarin fruit
633 by vis/NIR spectroscopy. *J. Near Infrared Spectrosc.* **2003**, *11*, 323–332, doi:10.1255/jnirs.383.
- 634 66. Greensill, C. V.; Walsh, K. B. Calibration transfer between miniature photodiode array-based
635 spectrometers in the near infrared assessment of mandarin soluble solids content. *J. Near Infrared
636 Spectrosc.* **2002**, *10*, 27–36.
- 637 67. Gómez, A. H.; He, Y.; Pereira, A. G. Non-destructive measurement of acidity, soluble solids and firmness
638 of Satsuma mandarin using Vis/NIR-spectroscopy techniques. *J. Food Eng.* **2006**, *77*, 313–319,
639 doi:http://dx.doi.org/10.1016/j.jfoodeng.2005.06.036.
- 640 68. Guthrie, J. A.; Reid, D. J.; Walsh, K. B. Assessment of internal quality attributes of mandarin fruit. 2. NIR
641 calibration model robustness. *Aust. J. Agric. Res.* **2005**, *56*, 417–426, doi:10.1071/AR04299.
- 642 69. Crisosto, C. H.; Crisosto, G. M.; Ritenour, M. A. Testing the reliability of skin color as an indicator of
643 quality for early season “Brooks” (*Prunus avium* L.) cherry. *Postharvest Biol. Technol.* **2002**, *24*, 147–154,
644 doi:10.1016/S0925-5214(01)00190-9.
- 645 70. Lu, R. Predicting Firmness and Sugar Content of Sweet Cherries Using Near-Infrared Diffuse Reflectance
646 Spectroscopy. *Trans. Am. Soc. Agric. Eng.* **2001**, *44*, 1265–1271, doi:10.13031/2013.6421.
- 647 71. Carlini, P.; Massantini, R.; Mencarelli, F. Vis-NIR measurement of soluble solids in cherry and apricot by
648 PLS regression and wavelength selection. *J. Agric. Food Chem.* **2000**, *48*, 5236–5242, doi:10.1021/jf000408f.
- 649 72. Sánchez, M. T.; De La Haba, M. J.; Benítez-López, M.; Fernández-Novales, J.; Garrido-Varo, A.; Pérez-
650 Marín, D. Non-destructive characterization and quality control of intact strawberries based on NIR
651 spectral data. *J. Food Eng.* **2012**, *110*, 102–108, doi:10.1016/j.jfoodeng.2011.12.003.

- 652 73. Amodio, M. L.; Ceglie, F.; Chaudhry, M. M. A.; Piazzolla, F.; Colelli, G. Potential of NIR spectroscopy for
653 predicting internal quality and discriminating among strawberry fruits from different production
654 systems. *Postharvest Biol. Technol.* **2017**, *125*, 112–121, doi:10.1016/j.postharvbio.2016.11.013.
- 655 74. Liu, C.; Liu, W.; Lu, X.; Ma, F.; Chen, W.; Yang, J.; Zheng, L. Application of multispectral imaging to
656 determine quality attributes and ripeness stage in strawberry fruit. *PLoS One* **2014**, *9*, e87818,
657 doi:10.1371/journal.pone.0087818.
- 658 75. ElMasry, G.; Wang, N.; ElSayed, A.; Ngadi, M. Hyperspectral imaging for nondestructive determination
659 of some quality attributes for strawberry. *J. Food Eng.* **2007**, *81*, 98–107, doi:10.1016/j.jfoodeng.2006.10.016.
- 660 76. Muhua, L.; Peng, F.; Renfa, C. Non destructive estimation peach SSC and firmness by mutispectral
661 reflectance imaging. *New Zeal. J. Agric. Res.* **2007**, *50*, 601–608, doi:10.1080/00288230709510328.
- 662 77. Tallada, J. G.; Nagata, M.; Kobayashi, T. Non-destructive estimation of firmness of strawberries (*Fragaria*
663 *x ananassa* Duch.) using NIR hyperspectral imaging. *Environ. Control Biol.* **2006**, *44*, 245–255.
- 664 78. Camps, C.; Christen, D. Non-destructive assessment of apricot fruit quality by portable visible-near
665 infrared spectroscopy. *LWT - Food Sci. Technol.* **2009**, *42*, 1125–1131, doi:10.1016/j.lwt.2009.01.015.
- 666 79. Slaughter, D. C.; Crisosto, C. H. Nondestructive internal quality assessment of kiwifruit using near-
667 infrared spectroscopy. *Semin. Food Anal.* **1998**, *3*, 131–140.
- 668 80. Lee, J.; Kim, S.; Seong, K.; Kim, C.; Um, Y.; Lee, S. Quality prediction of kiwifruit based on near infrared
669 spectroscopy. *Korean J. Hortic. Sci. Technol.* **2012**, *30*, 709–717.
- 670 81. McGlone, V. A.; Kawano, S. Firmness, dry-matter and soluble-solids assessment of postharvest kiwifruit
671 by NIR spectroscopy. *Postharvest Biol. Technol.* **1998**, *13*, 131–141, doi:10.1016/S0925-5214(98)00007-6.
- 672 82. Jannok, P.; Kamitani, Y.; Kawano, S. Development of a common calibration model for determining the
673 Brix value of intact apple, pear and persimmon fruits by near infrared spectroscopy. *J. Near Infrared*
674 *Spectrosc.* **2014**, *22*, 367–373, doi:10.1255/jnirs.1130.
- 675 83. Wei, X.; Liu, F.; Qiu, Z.; Shao, Y.; He, Y. Ripeness Classification of Astringent Persimmon Using
676 Hyperspectral Imaging Technique. *Food Bioprocess Technol.* **2014**, *7*, 1371–1380, doi:10.1007/s11947-013-
677 1164-y.
- 678 84. Omar, A. F. Spectroscopic profiling of soluble solids content and acidity of intact grape , lime , and star
679 fruit. *Sens. Rev.* **2013**, *3*, 238–245, doi:10.1108/02602281311324690.
- 680 85. Janik, L. J.; Cozzolino, D.; Damberg, R.; Cynkar, W.; Gishen, M. The prediction of total anthocyanin
681 concentration in red-grape homogenates using visible-near-infrared spectroscopy and artificial neural
682 networks. *Anal. Chim. Acta* **2007**, *594*, 107–118.
- 683 86. Agati, G.; D'Onofrio, C.; Ducci, E.; Cuzzola, A.; Remorini, D.; Tuccio, L.; Lazzini, F.; Mattii, G. Potential of
684 a multiparametric optical sensor for determining in situ the maturity components of red and white vitis
685 vinifera wine grapes. *J. Agric. Food Chem.* **2013**, *61*, 12211–12218, doi:10.1021/jf405099n.
- 686 87. Lenk, S.; Buschmann, C.; Pfündel, E. E. In vivo assessing flavonols in white grape berries (*Vitis vinifera* L.
687 cv. Pinot Blanc) of different degrees of ripeness using chlorophyll fluorescence imaging. *Funct. Plant Biol.*
688 **2007**, *34*, 1092–1104.
- 689 88. Baiano, A.; Terracone, C.; Peri, G.; Romaniello, R. Application of hyperspectral imaging for prediction of
690 physico-chemical and sensory characteristics of table grapes. *Comput. Electron. Agric.* **2012**, *87*, 142–151,
691 doi:10.1016/j.compag.2012.06.002.
- 692 89. Abu Bakar, B. H.; Ishak, A. J.; Shamsuddin, R.; Wan Hassan, W. Z. Ripeness level classification for
693 pineapple using RGB and HSI colour maps. *J. Theor. Appl. Inf. Technol.* **2013**, *57*, 587–593.
- 694 90. Guthrie, J.; Walsh, K. Non-invasive assessment of pineapple and mango fruit quality using near infra-red
695 spectroscopy. *Aust. J. Exp. Agric.* **1997**, *37*, 253–263.
- 696 91. Chia, K. S.; Abdul Rahim, H.; Abdul Rahim, R. Prediction of soluble solids content of pineapple via non-
697 invasive low cost visible and shortwave near infrared spectroscopy and artificial neural network. *Biosyst.*
698 *Eng.* **2012**, *113*, 158–165, doi:10.1016/j.biosystemseng.2012.07.003.
- 699 92. Infante, R.; Contador, L.; Rubio, P.; Mesa, K.; Meneses, C. Non-destructive monitoring of flesh softening
700 in the black-skinned Japanese plums “Angelino” and “Autumn beaut” on-tree and postharvest.
701 *Postharvest Biol. Technol.* **2011**, *61*, 35–40, doi:10.1016/j.postharvbio.2011.01.003.
- 702 93. Paz, P.; Sánchez, M. T.; Pérez-Marín, D.; Guerrero, J. E.; Garrido-Varo, A. Nondestructive determination
703 of total soluble solid content and firmness in plums using near-infrared reflectance spectroscopy. *J. Agric.*
704 *Food Chem.* **2008**, *56*, 2565–2570, doi:10.1021/jf073369h.
- 705 94. Mendoza, F. AND Aguilera, J. M. Application of Image Analysis for Classification of Ripening Bananas.

- 706 *Food Eng. Phys. Prop.* **2004**, *69*, 478–487.
- 707 95. M. OLMO, A. NADAS, A. J. M. G. Nondestructive Methods to Evaluate Maturity Level of Oranges. *Sens.*
708 *Nutr. Qual. Food Nondestruct.* **1998**, *65*, 365–369.
- 709 96. R.L. SHEWFELT, C.N. THAI, and J. W. D. Prediction of changes in color of tomatoes during ripening at
710 different constant temperatures. *J. Food Sci.* **1988**, *53*, 1433.
- 711 97. Mercado-Silva, E.; Benito-Bautista, P.; De los Angeles Garc??a-Velasco, M. Fruit development, harvest
712 index and ripening changes of guavas produced in central Mexico. *Postharvest Biol. Technol.* **1998**, *13*, 143–
713 150, doi:10.1016/S0925-5214(98), 3-9.
- 714 98. Shinya, P.; Contador, L.; Predieri, S.; Rubio, P.; Infante, R. Peach ripening: Segregation at harvest and
715 postharvest flesh softening. *Postharvest Biol. Technol.* **2013**, *86*, 472–478,
716 doi:10.1016/j.postharvbio.2013.07.038.
- 717 99. Luchsinger, L. E.; Walsh, C. S. Development of an objective and non-destructive harvest maturity index
718 for peaches and nectarines. *Acta Hort.* **1998**, *465*, 679–687.
- 719 100. Raut, K.; Bora, V. Assessment of Fruit Maturity using Digital Image Processing. *Int. J. Sci. Technol. Eng.*
720 **2016**, *3*, 273–279.
- 721 101. Taghadomi-Saberi, S.; Omid, M.; Emam-Djomeh, Z.; Faraji-Mahyari, K. H. Determination of cherry color
722 parameters during ripening by artificial neural network assisted image processing technique. *J. Agric. Sci.*
723 *Technol.* **2015**, *17*, 589–600.
- 724 102. Hobson, G. E.; Adams, P.; Dixon, T. J. Assessing the colour of tomato fruit during ripening. *J. Sci. Food*
725 *Agric.* **1983**, *34*, 286–292, doi:10.1002/jfsa.2740340312.
- 726 103. Andrés F. López Camelo; Perla A. Gómez Comparison of color indexes for tomato ripening. *Hortic. Bras.*
727 *Brasília*, **2004**, *22*, 534–537, doi:10.1590/S0102-05362004000300006.
- 728 104. Wu, D.; Sun, D. W. Colour measurements by computer vision for food quality control - A review. *Trends*
729 *Food Sci. Technol.* **2013**, *29*, 5–20, doi:10.1016/j.tifs.2012.08.004.
- 730 105. Tijsskens, L. M. M.; Evelo, R. G. Modelling colour of tomatoes during postharvest storage. *Postharvest Biol.*
731 *Technol.* **1994**, *4*, 85–98, doi:10.1016/0925-5214(94)90010-8.
- 732 106. Arias, R.; Lee, T.-C.; Logendra, L.; Janes, H. Correlation of Lycopene Measured by HPLC with the L*, a*,
733 b* Color Readings of a Hydroponic Tomato and the Relationship of Maturity with Color and Lycopene
734 Content. *J. Agric. Food Chem.* **2000**, *48*, 1697–1702, doi:10.1021/jf990974e.
- 735 107. Brandt, S.; Pék, Z.; Barna, É.; Lugasi, A.; Helyes, L. Lycopene content and colour of ripening tomatoes as
736 affected by environmental conditions. *J. Sci. Food Agric.* **2006**, *86*, 568–572, doi:10.1002/jfsa.2390.
- 737 108. D'Souza, M. C.; Singha, S.; Ingle, M. Lycopene Concentration of Tomato Fruit can be Estimated from
738 Chromaticity Values. *HortScience* **1992**, *27*, 465–466.
- 739 109. Jiménez-Cuesta, M.; Cuquerella, J.; Martínez-Javaga, J. M. Determination of a color index for citrus fruit
740 degreening. In *Proceedings of the International Society of Citriculture* [International Citrus Congress, November
741 9-12, 1981, Tokyo, Japan; K. Matsumoto, editor]; Shimizu, Japan: International Society of Citriculture, 1982-
742 1983., 1982.
- 743 110. Yam, K. L.; Papadakis, S. E. A simple digital imaging method for measuring and analyzing color of food
744 surfaces. *J. Food Eng.* **2004**, *61*, 137–142, doi:10.1016/S0260-8774(03)00195-X.
- 745 111. León, K.; Mery, D.; Pedreschi, F.; León, J. Color measurement in L*a*b* units from RGB digital images.
746 *Food Res. Int.* **2006**, *39*, 1084–1091, doi:10.1016/j.foodres.2006.03.006.
- 747 112. Klir, G.; Yuan, B. *Fuzzy sets and fuzzy logic*; Prentice hall New Jersey, 1995; Vol. 4.
- 748 113. Mansor, A. R.; Othman, M.; Ahmad, K. A.; Nazari, M.; Bakar, A.; Razak, T. R. Fuzzy RGB Colour Sensor
749 Model For Mango Ripening Index. *2013 IEEE Symp. Humanit. Sci. Eng. Res.* **2013**, 118–123.
- 750 114. Goel, N.; Sehgal, P. Fuzzy classification of pre-harvest tomatoes for ripeness estimation - An approach
751 based on automatic rule learning using decision tree. *Appl. Soft Comput. J.* **2015**, *36*, 45–56,
752 doi:10.1016/j.asoc.2015.07.009.
- 753 115. Hartigan, J. A.; Wong, M. A. Algorithm AS 136: A k-means clustering algorithm. *J. R. Stat. Soc. Ser. C*
754 *(Applied Stat.)* **1979**, *28*, 100–108.
- 755 116. Lesot, M.-J.; Kruse, R. Gustafson-Kessel-like clustering algorithm based on typicality degrees. *Int. Conf.*
756 *Inf. Process. Manag. Uncertain. Knowledge-Based Syst.* **2006**, 1300–1307.
- 757 117. Niño-Medina, G.; Rivera-Castro, J. C.; Vidales-Contreras, J. A.; Rodriguez-Fuentes, H.; Luna-Maldonado,
758 A. I. PhysicoChemical Parameters for Obtaining Prediction Models in the Postharvest Quality of
759 Tomatoes (*Solanum Lycopersicum* L.). *Mda* **2013**, *6*, 54–66.

- 760 118. Takahashi, N.; Maki, H.; Nishina, H.; Takayama, K. *Evaluation of Tomato Fruit Color Change with Different*
761 *Maturity Stages and Storage Temperatures Using Image Analysis*; IFAC, 2013; Vol. 46:.
- 762 119. Yanai, H.; Mayekawa, S. ichi Review of Linear Algebra and Linear Models by R.B. Bapat. *Linear Algebra*
763 *Appl.* **1994**, *207*, 273–277, doi:10.1016/0024-3795(94)90014-0.
- 764 120. Jain, A. K.; Mao, J. Artificial Neural Network: A Tutorial. *Communications* **1996**, *29*, 31–44,
765 doi:10.1109/2.485891.
- 766 121. Hartmann, A.; Czauderna, T.; Hoffmann, R.; Stein, N.; Schreiber, F. HTPPheno: An image analysis pipeline
767 for high-throughput plant phenotyping. *BMC Bioinformatics* **2011**, *12*, 148, doi:10.1186/1471-2105-12-148.
- 768 122. Segmentation and Histogram Generation Using the Hsv Color Space for. **2002**, 589–592.
- 769 123. Ukirade, N. S. Color Grading System for Evaluating Tomato Maturity. **2014**, *2*, 41–45.
- 770 124. Singh, M.; Markou, M.; Singh, S. Colour image texture analysis: dependence on colour spaces. *Object*
771 *Recognit. Support. by user Interact. Serv. Robot.* **2002**, *1*, 672–675, doi:10.1109/ICPR.2002.1044842.
- 772 125. Duda, R. O.; Hart, P. E.; Stork, D. G. *Pattern classification*; John Wiley & Sons, 2012; ISBN 111858600X.
- 773 126. Li, H.; Lee, W. S.; Wang, K. Identifying blueberry fruit of different growth stages using natural outdoor
774 color images. *Comput. Electron. Agric.* **2014**, *106*, 91–101, doi:10.1016/j.compag.2014.05.015.
- 775 127. Tarkosova, J.; Copikova, J. Determination of carbohydrate content in bananas during ripening and
776 storage by near infrared spectroscopy. *J. Near Infrared Spectrosc.* **2000**, *8*, 21–26, doi:10.1255/jnirs.260.
- 777 128. Makky, M.; Soni, P. In situ quality assessment of intact oil palm fresh fruit bunches using rapid portable
778 non-contact and non-destructive approach. *J. Food Eng.* **2014**, *120*, 248–259,
779 doi:10.1016/j.jfoodeng.2013.08.011.
- 780 129. Lleo, L.; Roger, J. M.; Herrero-Langreo, A.; Diezma-Iglesias, B.; Barreiro, P. Comparison of multispectral
781 indexes extracted from hyperspectral images for the assessment of fruit ripening. *J. Food Eng.* **2011**, *104*,
782 612–620, doi:10.1016/j.jfoodeng.2011.01.028.
- 783 130. Ruiz-Altisent, M.; Lleo, L.; Riquelme, F. Instrumental quality assessment of peaches: Fusion of optical and
784 mechanical parameters. *J. Food Eng.* **2006**, *74*, 490–499, doi:10.1016/j.jfoodeng.2005.01.048.
- 785 131. Ziosi, V.; Noferini, M.; Fiori, G.; Tadiello, A.; Trainotti, L.; Casadoro, G.; Costa, G. A new index based on
786 vis spectroscopy to characterize the progression of ripening in peach fruit. *Postharvest Biol. Technol.* **2008**,
787 *49*, 319–329, doi:10.1016/j.postharvbio.2008.01.017.
- 788 132. Lurie, S.; Friedman, H.; Weksler, A.; Dagar, A.; Eccher Zerbini, P. Maturity assessment at harvest and
789 prediction of softening in an early and late season melting peach. *Postharvest Biol. Technol.* **2013**, *76*, 10–16,
790 doi:10.1016/j.postharvbio.2012.08.007.
- 791 133. Costa, g.; Noferini, m; Fiori, G; Ziosi, V; Berthod, N; Rossier, J. Establishment of the optimal harvest time
792 in agricot ('Orangered' and 'Bergarouge') by means of a new index based on vis spectroscopy. In *Acta*
793 *Horticulturae*; International Society for Horticultural Science (ISHS), Leuven, Belgium, 2010; pp. 533–539.
- 794 134. Costa, G.; Noferini, M.; Fiori, G.; Torrigiani, P. Use of Vis / NIR Spectroscopy to Assess Fruit Ripening
795 Stage and Improve Management in Post-Harvest Chain. *Fresh Prod.* **2009**, *3*, 35–41.
- 796 135. Bonora, E.; Noferini, M.; Stefanelli, D.; Costa, G. A new simple modeling approach for the early
797 prediction of harvest date and yield in nectarines. *Sci. Hortic. (Amsterdam)*. **2014**, *172*, 1–9,
798 doi:10.1016/j.scienta.2014.03.030.
- 799 136. Helland, I. Partial least squares regression. *Encycl. Stat. Sci.* **2006**.
- 800 137. Mahesh, S.; Jayas, D. S.; Paliwal, J.; White, N. D. G. Comparison of Partial Least Squares Regression
801 (PLSR) and Principal Components Regression (PCR) Methods for Protein and Hardness Predictions using
802 the Near-Infrared (NIR) Hyperspectral Images of Bulk Samples of Canadian Wheat. *Food Bioprocess*
803 *Technol.* **2014**, *8*, 31–40, doi:10.1007/s11947-014-1381-z.
- 804 138. Gómez, A. H.; He, Y.; Pereira, A. G. Non-destructive measurement of acidity, soluble solids and firmness
805 of Satsuma mandarin using Vis/NIR-spectroscopy techniques. *J. Food Eng.* **2006**, *77*, 313–319,
806 doi:http://dx.doi.org/10.1016/j.jfoodeng.2005.06.036.
- 807 139. Park, B.; Abbott, J. A.; Lee, K. J.; Choi, C. H.; Choi, K. H. N Near-infrared diffuse reflectance for
808 quantitative and qualitative measurement soluble solids and firmness of Delicious and Gala apples.
809 *Trans. ASAE* **2003**, *46*, 1721–1731, doi:10.13031/2013.15628.
- 810 140. He, Y.; Zhang, Y.; Pereira, A. G.; Gómez, A. H.; Wang, J. Nondestructive Determination of Tomato Fruit
811 Quality Characteristics Using Vis / NIR Spectroscopy Technique. *Int. J. Inf. Technol.* **2005**, *11*, 97–108.
- 812 141. Mollazade, K.; Omid, M.; Tab, F. A.; Mohtasebi, S. S. Principles and Applications of Light Backscattering
813 Imaging in Quality Evaluation of Agro-food Products: A Review. *Food Bioprocess Technol.* **2012**, *5*, 1465–

- 814 1485, doi:10.1007/s11947-012-0821-x.
- 815 142. Rinnan, A.; Berg, F. van den; Engelsen, S. B. Review of the most common pre-processing techniques for
816 near-infrared spectra. *TrAC - Trends Anal. Chem.* 2009, 28, 1201–1222.
- 817 143. Herrera, J.; Guesalaga, a; Agosin, E. Shortwave near infrared spectroscopy for non-destructive
818 determination of maturity of wine grapes. *Meas. Sci. Technol.* 2003, 14, 689–697, doi:10.1088/0957-
819 0233/14/5/320.
- 820 144. Guo, Z.; Huang, W.; Chen, L.; Wang, X.; Peng, Y. Nondestructive evaluation of soluble solid content in
821 strawberry by near infrared spectroscopy. *Third Int. Conf. Photonics Image Agric. Eng. (PIAGENG 2013)*
822 2013, 8761, 876100–876100, doi:10.1117/12.2019628.
- 823 145. Gorry, P. A. General least-squares smoothing and differentiation by the convolution (Savitzky-Golay)
824 method. *Anal. Chem.* 1990, 62, 570–573.
- 825 146. Nicola, B. M.; Beullens, K.; Bobelyn, E.; Peirs, A.; Saeys, W.; Theron, K. I.; Lammertyn, J. Nondestructive
826 measurement of fruit and vegetable quality by means of NIR spectroscopy: A review. *Postharvest Biol.*
827 *Technol.* 2007, 46, 99–118, doi:10.1016/j.postharvbio.2007.06.024.
- 828 147. Marques, E. J. N.; De Freitas, S. T.; Pimentel, M. F.; Pasquini, C. Rapid and non-destructive determination
829 of quality parameters in the “Tommy Atkins” mango using a novel handheld near infrared spectrometer.
830 *Food Chem.* 2016, 197, 1207–1214, doi:10.1016/j.foodchem.2015.11.080.
- 831 148. Torres, I.; Pérez-Marín, D.; De la Haba, M. J.; Sánchez, M. T. Fast and accurate quality assessment of Raf
832 tomatoes using NIRS technology. *Postharvest Biol. Technol.* 2015, 107, 9–15,
833 doi:10.1016/j.postharvbio.2015.04.004.
- 834 149. Saranwong, S.; Sornsrivichai, J.; Kawano, S. Prediction of ripe-stage eating quality of mango fruit from its
835 harvest quality measured nondestructively by near infrared spectroscopy. *Postharvest Biol. Technol.* 2004,
836 31, 137–145, doi:10.1016/j.postharvbio.2003.08.007.
- 837 150. Ma, G.; Fu, X.; Zhou, Y.; Ying, Y.; Xu, H.; Xie, L.; Lin, T. Nondestructive sugar content determination of
838 peaches by using near infrared spectroscopy technique. *Guang pu xue yu guang pu fen xi* 2007, 27, 907–
839 910.
- 840 151. Dhanoa, M.; Lister, S.; Sanderson, R.; Barnes, R. The link between multiplicative scatter correction (MSC)
841 and standard normal variate (SNV) transformations of NIR spectra. *J. Near Infrared Spectrosc.* 1994, 2, 43,
842 doi:10.1255/jnirs.30.
- 843 152. Nishizawa, T.; Mori, Y.; Fukushima, S.; Natsuga, M.; Maruyama, Y. Non-destructive analysis of soluble
844 sugar components in strawberry fruits using near-infrared spectroscopy. *Nippon Shokuhin Kagaku Kogaku*
845 *Kaishi* 2009, 56, 229–235, doi:10.3136/nshkk.56.229.
- 846 153. Peiris Dull, G. G.; Leffler, R. G.; Kays, S.J., K. H. S. Near-infrared spectrometric method for nondestructive
847 determination of soluble solids content of peaches. *J. Am. Soc. Hortic. Sci.* 1998, 123, 898–905.
- 848 154. Clément, A.; Dorais, M.; Vernon, M. Multivariate approach to the measurement of tomato maturity and
849 gustatory attributes and their rapid assessment by vis-NIR spectroscopy. *J. Agric. Food Chem.* 2008, 56,
850 1538–1544, doi:10.1021/jf072182n.
- 851 155. Saranwong, S.; Sornsrivichai, J.; Kawano, S. Improvement of PLS calibration for Brix value and dry matter
852 of mango using information from MLR calibration. *J. Near Infrared Spectrosc.* 2001, 9, 287–295,
853 doi:10.1255/jnirs.314.
- 854 156. Kawano, S.; Watanabe, H.; Iwamoto, M. Determination of Sugar Content in Intact Peaches by Near
855 Infrared Spectroscopy with Fiber Optics in Interactance Mode. *J. Japanese Soc. Hortic. Sci.* 1992, 61, 445–
856 451, doi:10.2503/jjshs.61.445.
- 857 157. Jiang, M.; Lu, H.; Ying, Y.; Xu, H. Design and validation of software for real-time soluble solids content
858 evaluation of peach by near infrared spectroscopy. 2006, 6381, 638118, doi:10.1117/12.686480.
- 859 158. Guthrie, J.; Wedding, B.; Walsh, K. Robustness of NIR calibrations for soluble solids in intact melon and
860 pineapple. *J. Near Infrared Spectrosc.* 1998, 6, 259–265, doi:10.1255/jnirs.145.
- 861 159. Ouyang, A.-G. Partial least squares regression variable screening studies on apple soluble solids nir
862 spectral detection. *Spectrosc. Spectr. Anal.* 2012, 32, 2680–2684.
- 863 160. Jha, S. N.; Narsaiah, K.; Jaiswal, P.; Bhardwaj, R.; Gupta, M.; Kumar, R.; Sharma, R. Nondestructive
864 prediction of maturity of mango using near infrared spectroscopy. *J. Food Eng.* 2014, 124, 152–157,
865 doi:10.1016/j.jfoodeng.2013.10.012.
- 866 161. Gracia, A.; Leon, L. Non-destructive assessment of olive fruit ripening by portable near infrared
867 spectroscopy. *Grasas Y Aceites* 2011, 62, 268–274, doi:10.3989/gya.089610.

- 868 162. Herold, B.; Truppel, I.; Zude, M.; Geyer, M. Spectral measurements on “Elstar” apples during fruit
869 development on the tree. *Biosyst. Eng.* **2005**, *91*, 173–182, doi:10.1016/j.biosystemseng.2005.03.005.
- 870 163. Bodria, L.; Fiala, M.; Guidetti, R.; Oberti, R. Optical techniques to estimate the ripeness of red-pigmented
871 fruits. *2004*, *47*(3), 815–820.
- 872 164. Royer, C. A. Fluorescence spectroscopy. *Methods Mol. Biol.* **1995**, *40*, 65–89, doi:10.1385/0-89603-301-5:65.
- 873 165. Song, J.; Deng, W.; Beaudry, R. M.; Armstrong, P. R. Changes in chlorophyll fluorescence of apple fruit
874 during maturation, ripening, and senescence. *HortScience* **1997**, *32*, 891–896.
- 875 166. Urbano Bron, I.; Vasconcelos Ribeiro, R.; Azzolini, M.; Pedro Jacomino, A.; Caruso MacHado, E.
876 Chlorophyll fluorescence as a tool to evaluate the ripening of “Golden” papaya fruit. *Postharvest Biol.*
877 *Technol.* **2004**, *33*, 163–173, doi:10.1016/j.postharvbio.2004.02.004.
- 878 167. Morales, F.; Cerovic, Z. G.; Moya, I. Time-resolved blue-green fluorescence of sugar beet (*Beta vulgaris* L.)
879 leaves. Spectroscopic evidence for the presence of ferulic acid as the main fluorophore of the epidermis.
880 *Biochim. Biophys. Acta - Bioenerg.* **1996**, *1273*, 251–262, doi:10.1016/0005-2728(95)00153-0.
- 881 168. Hazir, M. H. M.; Shariff, A. R. M.; Amiruddin, M. D.; Ramli, A. R.; Iqbal Saripan, M. Oil palm bunch
882 ripeness classification using fluorescence technique. *J. Food Eng.* **2012**, *113*, 534–540,
883 doi:10.1016/j.jfoodeng.2012.07.008.
- 884 169. ElMasry, G. M.; Nakauchi, S. Image analysis operations applied to hyperspectral images for non-invasive
885 sensing of food quality - A comprehensive review. *Biosyst. Eng.* **2016**, *142*, 53–82,
886 doi:10.1016/j.biosystemseng.2015.11.009.
- 887 170. Mahesh, S.; Jayas, D. S.; Paliwal, J.; White, N. D. G. Hyperspectral imaging to classify and monitor quality
888 of agricultural materials. *J. Stored Prod. Res.* **2015**, *61*, 17–26, doi:10.1016/j.jspr.2015.01.006.
- 889 171. Bauriegel, E.; Giebel, a.; Geyer, M.; Schmidt, U.; Herppich, W. B. Early detection of *Fusarium* infection in
890 wheat using hyper-spectral imaging. *Comput. Electron. Agric.* **2011**, *75*, 304–312,
891 doi:10.1016/j.compag.2010.12.006.
- 892 172. Zhao, Y.; Gong, L.; Huang, Y.; Liu, C. Robust tomato recognition for robotic harvesting using feature
893 images fusion. *Sensors (Switzerland)* **2016**, *16*, doi:10.3390/s16020173.
- 894 173. Honkavaara, E.; Kaivosoja, J.; Mäkynen, J.; Pellikka, I.; Pesonen, L.; Saari, H.; Salo, H.; Hakala, T.;
895 Marklelin, L.; Rosnell, T. Hyperspectral Reflectance Signatures and Point Clouds for Precision
896 Agriculture By Light Weight Uav Imaging System. *ISPRS Ann. Photogramm. Remote Sens. Spat. Inf. Sci.*
897 **2012**, *I-7*, 353–358, doi:10.5194/isprsannals-I-7-353-2012.
- 898 174. Mendoza, F.; Lu, R.; Ariana, D.; Cen, H.; Bailey, B. Integrated spectral and image analysis of
899 hyperspectral scattering data for prediction of apple fruit firmness and soluble solids content. *Postharvest*
900 *Biol. Technol.* **2011**, *62*, 149–160, doi:10.1016/j.postharvbio.2011.05.009.
- 901 175. Centner, V.; Massart, D.-L.; de Noord, O. E.; de Jong, S.; Vandeginste, B. M.; Sterna, C. Elimination of
902 uninformative variables for multivariate calibration. *Anal. Chem.* **1996**, *68*, 3851–3858.
- 903 176. Zhu, Q.; Huang, M.; Zhao, X.; Wang, S. Wavelength selection of hyperspectral scattering image using
904 new semi-supervised affinity propagation for prediction of firmness and soluble solid content in apples.
905 *Food Anal. Methods* **2013**, *6*, 334–342.
- 906 177. Wang, S.; Huang, M.; Zhu, Q. Model fusion for prediction of apple firmness using hyperspectral
907 scattering image. *Comput. Electron. Agric.* **2012**, *80*, 1–7, doi:10.1016/j.compag.2011.10.008.
- 908 178. ElMasry, G.; Wang, N.; ElSayed, A.; Ngadi, M. Hyperspectral imaging for nondestructive determination
909 of some quality attributes for strawberry. *J. Food Eng.* **2007**, *81*, 98–107, doi:10.1016/j.jfoodeng.2006.10.016.
- 910 179. Leiva-Valenzuela, G. a.; Lu, R.; Aguilera, J. M. Prediction of firmness and soluble solids content of
911 blueberries using hyperspectral reflectance imaging. *J. Food Eng.* **2013**, *115*, 91–98,
912 doi:10.1016/j.jfoodeng.2012.10.001.
- 913 180. Araujo, Mario Cesar Ugulino, Teresa Cristina Bezerra Saldanha, R. K. H. G. 1; ~; Yoneyama1, T.; Chame,
914 H. C.; Valeria The successive projections algorithm for variable selection in spectroscopic
915 multicomponent analysis. *Chemom. Intell. Lab. Syst.* **2001**, doi:10.1016/S0169-7439(01)00119-8.
- 916 181. Peng, Y.; Lu, R. An LCTF-based multispectral imaging system for estimation of apple fruit firmness::
917 PART I. Acquisition and characterization of scattering images.
918 *Trans. ASABE* **2006**, *49*, 269–275, doi:10.13031/2013.20224.
- 919 182. Saeed, O. M. Ben; Sankaran, S.; Shariff, A. R. M.; Shafri, H. Z. M.; Ehsani, R.; Alfatni, M. S.; Hazir, M. H.
920 M. Classification of oil palm fresh fruit bunches based on their maturity using portable four-band sensor
921 system. *Comput. Electron. Agric.* **2012**, *82*, 55–60, doi:10.1016/j.compag.2011.12.010.

- 922 183. Yang, H. Remote sensing technique for predicting harvest time of tomatoes. *Procedia Environ. Sci.* **2011**, *10*,
923 666–671, doi:10.1016/j.proenv.2011.09.107.
- 924 184. Peirs, A.; Lammertyn, J.; Ooms, K.; Nicola, B. M. Prediction of the optimal picking date of different apple
925 cultivars by means of VIS/NIR-spectroscopy. *Postharvest Biol. Technol.* **2001**, *21*, 189–199,
926 doi:10.1016/S0925-5214(00)00145-9.
- 927 185. Teng, L.; Cheng, Z.; Chen, X.; Lai, L. Study on simulation models of tomato fruit quality related to
928 cultivation environmental factors. *Acta Ecol. Sin.* **2012**, *32*, 111–116, doi:10.1016/j.chnaes.2012.02.001.
- 929 186. Loomis, R. S.; Williams, W. A. Maximum crop productivity: an estimate. *Crop Sci.* **1963**, *3*, 67–72.
- 930 187. JonesCA, K. R. CERES2Maize: A simulation model of maize growth and development. *Texas A & M Univ.*
931 *Press. Coll. Stn.* **1986**.
- 932 188. Whisler, F. D.; Acock, B.; Baker, D. N.; Fye, R. E.; Hodges, H. F.; Lambert, J. R.; Lemmon, H. E.; McKinion,
933 J. M.; Reddy, V. R. Crop simulation models in agronomic systems. *Adv. Agron.* **1986**, *40*, 141–208.
- 934 189. Yang, H.; Dobermann, A.; Cassman, K. G.; Walters, D. T. Features, applications, and limitations of the
935 hybrid-maize simulation model. *Agron. J.* **2006**, *98*, 737–748, doi:10.2134/agronj2005.0162.
- 936 190. Jones, J. W.; Dayan, E.; Allen, L. H.; Van Keulen, H.; Challa, H. A dynamic tomato growth and yield
937 model (Tomgro). *Trans. ASAE* **1991**, *34*, 0663–0672, doi:10.13031/2013.31715.
- 938 191. Gijzen, H.; Heuvelink, E.; Challa, H.; Dayan, E.; Marcelis, L. F. M.; Cohen, S.; Fuchs, M. Hortisim: A
939 model for greenhouse crops and greenhouse climate. *Acta Hort.* **1998**, *456*, 441–450.
- 940 192. Qiu, Q.; Shi, K.; Qiao, X. J.; Jiang, K. Determining the Dominant Environmental Parameters for
941 Greenhouse Tomato Seedling Growth Modeling Using Canonical Correlation Analysis. *IFAC-*
942 *PapersOnLine* **2016**, *49*, 387–391, doi:10.1016/j.ifacol.2016.10.071.
- 943 193. Tomana, T.; Utsunomiya, N.; Kataoka, I. The effect of environmental temperatures on fruit ripening on
944 the tree II. The effect of temperatures around whole vines and clusters on the coloration of “Kyoho”
945 grapes. *J. Japanese Soc. Hortic. Sci.* **1979**, *48*, 261–266, doi:10.2503/jjshs.48.261.
- 946 194. Yamada, H.; Ohmura, H.; Arai, C.; Terui, M. Effect of preharvest fruit temperature on ripening, sugars,
947 and watercore occurrence in apples. *J. Am. Soc. Hortic. Sci.* **1994**, *119*, 1208–1214.
- 948 195. Medlicott, A. P.; Reynolds, S. B.; Thompson, A. K. Effects of Temperature on the Ripening of Mango. *J.*
949 *Sci. Food Agric.* **1986**, *37*, 469–474.
- 950 196. Braun, J. C. Effects of temperature and Propylene on apricot ripening. *Test.*
- 951 197. Cordenunsi, B. R.; Genovese, M. I.; Oliveira Do Nascimento, J. R.; Aymoto Hassimoto, N. M.; Jos?? Dos
952 Santos, R.; Lajolo, F. M. Effects of temperature on the chemical composition and antioxidant activity of
953 three strawberry cultivars. *Food Chem.* **2005**, *91*, 113–121, doi:10.1016/j.foodchem.2004.05.054.
- 954 198. Kawano, S.; Abe, H. Development of a calibration equation with temperature compensation for
955 determining the Brix value in intact peaches. **1995**, *218*, 211–218.
- 956 199. FAO *Global food losses and food waste - Extent, causes and prevention.*; 2011; ISBN 9789251072059.